IOPscience iopscience.iop.org

Home Search Collections Journals About Contact us My IOPscience

Shallow versus deep hydrogen states in ZnO and HgO

This article has been downloaded from IOPscience. Please scroll down to see the full text article.

2001 J. Phys.: Condens. Matter 13 9001

(http://iopscience.iop.org/0953-8984/13/40/316)

View the table of contents for this issue, or go to the journal homepage for more

Download details:
IP Address: 171.66.16.226
The article was downloaded on 16/05/2010 at 14:56

Please note that terms and conditions apply.

INSTITUTE OF PHYSICS PUBLISHING JOURNAL OF PHYSICS: CONDENSED MATTER

J. Phys.: Condens. Matter **13** (2001) 9001–9010 PII: S0953-8984(01)24941-8

Shallow versus deep hydrogen states in ZnO and HgO

S F J Cox[1,2], E A Davis[3], P J C King[1], J M Gil[4], H V Alberto[4], R C Vilão[4], J Piroto Duarte[4], N Ayres de Campos[4] and R L Lichti[5]

[1] ISIS Facility, Rutherford Appleton Laboratory, Chilton OX11 0QX, UK
[2] Department of Physics and Astronomy, University College London, London WCE 6BT, UK
[3] Department of Physics and Astronomy, University of Leicester, Leicester LEI 7RH, UK
[4] Physics Department, University of Coimbra, P-3004-516 Coimbra, Portugal
[5] Physics Department, Texas Tech University, Lubbock, TX 79409-1051, USA

Received 21 March 2001
Published 20 September 2001
Online at stacks.iop.org/JPhysCM/13/9001

Abstract

The muonium states mimicking interstitial hydrogen in ZnO and HgO are compared. Whereas in ZnO a theoretically predicted shallow donor state is confirmed, in HgO we find a considerably deeper state. The respective ionization temperatures are around 40 K and 150 K and the donor ionization energies are 19 ± 1 and 136 ± 3 meV, deduced from the temperature dependence of the μSR (muon spin-rotation) signal amplitudes. The μSR spectra provide a comprehensive characterization of the undissociated paramagnetic states: the hyperfine parameters, which measure the electron spin density on and near the muon, differ by a factor of $\sim$30. These define a hydrogenic radius of 1.1 nm in ZnO but indicate a much more compact electronic wavefunction in HgO, more akin to those of Mu* and the AA9 centre in Si. These data should largely carry over to hydrogen as a guide to its electrical activity in these materials.

1. Introduction: donor and acceptor states of interstitial hydrogen

Isolated hydrogen centres, notably trapped interstitial hydrogen atoms, are hard to detect and study in semiconductors by conventional spectroscopies. This is despite the fact that hydrogen is a common impurity which may be present in substantial concentrations—virtually unavoidable in material derived from hydride or organic precursors. The reason is twofold. Firstly, the interstitial atoms are believed to constitute negative-U centres, so there is no position of the Fermi level that stabilizes the neutral paramagnetic centres. Secondly, hydrogen diffuses so readily and is so reactive that it is invariably found paired with other defects or impurities: this is the origin of electrical passivation, whether of unwanted dangling bonds or interfacial defects or—less desirably—of deliberate dopants [1]. Nonetheless the isolated states are likely to play a role in diffusion and as precursors to passivation complexes. Their role undoubtedly becomes significant at temperatures where the passivation complexes dissociate. Best known is

their amphoteric behaviour as deep donors and acceptors. This is well documented in Si, where techniques such as deep-level transient spectroscopy give the relevant donor and acceptor levels as lying 0.2 and ~0.6 eV below the conduction band, respectively [2–5]. By comparison with shallow-donor or shallow-acceptor binding energies lying typically in the range 10–50 meV, these values confirm the long-standing view of hydrogen impurity as a deep-level defect in semiconductors.

An atomistic picture of the interplay of site and charge state that is responsible for this behaviour comes from direct spectroscopic observation of the muonium counterparts of the states involved [6–9], as summarized in section 2, and is substantiated by *ab initio* and other theoretical studies [1, 10–13]. In brief, the electrical activity of hydrogen is at present understood in terms of transitions between four main states, commonly denoted as H^+_{BC}, H^0_{BC}, H^-_T and H^0_T, where BC stands for the bond-centre site and T for the tetrahedral cage centre. The 0/+ donor level depth is defined by the ionization energy, without site change, of H^0_{BC}. Whereas there is some discussion as to which transition is monitored in particular experiments [5], it seems likely that the 0/− acceptor function involves an interplay between H^0_{BC} and H^-_T [8]; certainly a site change is required for negative-*U* behaviour [14].

In the group-IV elemental and III–V compound semiconductors, at least, hydrogen impurity acts only to counteract the prevailing conductivity—whether as a deep-level compensating defect or by formation of electrically inactive complexes [1]. In the II–VI compound ZnO, some early electrical measurements were taken as evidence that hydrogen could, in this wider-gap material, act as a dopant in its own right [15, 16]. This work seems largely to have been forgotten, or perhaps questions remained as to whether the behaviour represented activation of some other defect, until it was rediscovered in the light of present interest in the II–VI compounds for optoelectronic and photovoltaic applications. In our own studies of these materials, using muonium as a model for hydrogen, the observation that muonium defect centres in CdS have the spectroscopic and ionization characteristics of shallow donors [17] came as a surprise. However, in independent *ab initio* work, the shallow-donor behaviour for protium in ZnO has now been put on a firm theoretical footing [18]. Immediate confirmation of the muonium counterpart of this predicted state in ZnO and its observation in CdSe and CdTe as well as CdS [19] raise the question of how widespread the shallow donor states of hydrogen and muonium are amongst the II–VI compounds.

In this paper we present a fascinating contrast between the paramagnetic muonium states in ZnO and HgO and speculate on the issues raised. (In a comparison of the group-IIB oxides it would be natural to include CdO too but, as mentioned below, the paramagnetic muonium state is not formed in sufficient yield in our powder sample of this material.)

2. Methodology: muonium as a model for hydrogen

For observation of the neutral paramagnetic centres, muonium studies are at a particular advantage. Muonium[1] is commonly formed when positive muons are implanted at low temperatures in semiconductors, the initially energetic muons capturing electrons on thermalization. It may be detected and characterized with great sensitivity via μSR (muon spin-rotation) spectroscopy [6, 20], the short muon lifetime ($\tau_\mu \approx 2.2$ microseconds) setting a timescale which favours population of intrinsic interstitial sites, before diffusion occurs to other defects or impurities.

[1] Mu = $[\mu^+e^-]$ is the pseudo-isotope of hydrogen formed in its atomic state when the positive muon binds a single electron. The binding energy is the same as that of protium, i.e. 13.6 eV, to within a fraction of a per cent in the vacuum or free-atom state. As defect centres in semiconductors we denote the different possible charge states as Mu^+, Mu^0 and Mu^-, mimicking the interstitial proton, neutral hydrogen atom and hydride ion.

Even if muonium, like hydrogen, constitutes a negative-U system, these neutral paramagnetic centres and their hyperfine-coupled spin states are sufficiently long-lived—in pure material and below their respective ionization temperatures—for spectroscopic characterization. The muon–electron hyperfine interaction is the chief guide to local electronic structure, measured as described in section 3. Contrary to motional isotope effects, which may be large[2], neither hyperfine parameters nor energy-level differences are greatly sensitive to zero-point energy (this is about three times greater for Mu than for H in a harmonic potential well, since $m_{\mathrm{Mu}}/m_{\mathrm{H}} \approx 1/9$), so inferences concerning local electronic structure and electrical activity should carry over, *mutatis mutandis*, as a guide to the behaviour of protium [20].

3. Hyperfine spectroscopy: electronic structures

In intrinsic and lightly doped Si, both the bond-centred and cage-centred forms of paramagnetic muonium, $\mathrm{Mu}^0_{\mathrm{BC}}$ and $\mathrm{Mu}^0_{\mathrm{T}}$, are visible in the low-temperature μSR spectrum. Indeed it was the detection of their coexisting μSR signals which first indicated that more than one site and electronic structure for neutral hydrogen centres might exist [21]. Likewise it was the eventual assignment of the anisotropic spectrum that led to identification of the bond-centre site [22], then unanticipated[3] but now believed to be the more stable location for neutral hydrogen (and interstitial protons) in Si.

In sufficiently high magnetic fields, i.e. in the Paschen–Back régime, the μSR spectrum for neutral muonium appears as a doublet, split by the hyperfine interaction—the hyperfine field from the electron spin adding to or subtracting from the applied field, according to whether the electron spin is up or down. For $\mathrm{Mu}^0_{\mathrm{T}}$, the spectrum is isotropic and the hyperfine constant is a substantial fraction of the free-atom value. That is, most of the spin density is centred on the muon itself—this state has the characteristics of a muonium atom trapped in the interstitial cage (albeit highly mobile, diffusing between neighbouring cages). For $\mathrm{Mu}^0_{\mathrm{BC}}$, on the other hand, the hyperfine tensor has axial symmetry about the bond axis. This state is immobile in silicon up to its ionization temperature around 150 K [5]. Its principal values are expressed as isotropic and dipolar parameters in table 1, along with those for all the materials discussed in this paper, according to

$$A_{\mathrm{iso}} = \frac{1}{3}(A_{\parallel} + 2A_{\perp}) \tag{1}$$

$$D = \frac{2}{3}(A_{\parallel} - A_{\perp}). \tag{2}$$

[2] If diffusion involves a unique species—the elusive transport state— the individual mobilities of H and Mu would be very different. If, on the other hand, diffusion involves transitions between a highly mobile neutral state and essentially immobile ionic states, it is instead trap-limited and governed by capture and loss of charge carriers. It is then intimately linked with electrical activity and may well be similar for H and Mu.

[3] Known in the early literature as 'anomalous muonium' or Mu* [21, 6].

Table 1. Hyperfine parameters for muonium states in various semiconductors. A_{iso} = contact interaction (equation (1)); D = dipolar parameter (equation (2)); the units are MHz. (Values for Si, ZnSe and ZnS are taken from references [6] and [22]; the value of A_{iso} for free muonium, for comparison, is 4463 MHz.)

	ZnO	HgO	Si ($\mathrm{Mu_{BC}}$)	Si ($\mathrm{Mu_T}$)	ZnSe	ZnS
A_{iso}	0.5	15.0	−67	2066	3457	3548
D	0.26	5.2	51			

3.1. Deep states

The parameter $A_{\rm iso}$ in equation (1) is the contact interaction—a measure of electron spin density at the muon. For $\rm Mu^0_{BC}$ in Si this is in fact negative (representing polarization of the valence electrons) but the dipolar parameter D takes almost its maximum possible value, indicating that the unpaired electron is nonetheless localized nearby, at a distance of order 0.1 nm only. Chemical arguments as well as direct measurements of the spin density on ^{29}Si nuclei indicate that the electron spin is shared chiefly between the two nearest silicon atoms neighbouring the bond-centre site [22, 23]. In Si, the protium analogue is known to ESR spectroscopy as the AA9 centre [24, 25]. These species are best described as molecular radicals formed by chemical reaction of muonium or hydrogen with the Si lattice. Essentially the excess electron is accommodated in the antibonding orbital of the stretched Si–Si bond, so the singly occupied molecular orbital in fact has a node at the muon or proton site.

It is for Si that the correspondence between the electrically active donor and acceptor levels of muonium and hydrogen is best documented [5–9] but similar deep-level behaviour is known for muonium—and may be inferred for hydrogen—in other semiconductors. Thus trapped $\rm Mu^0_T$ atoms and the molecular radicals $\rm Mu^0_{BC}$ also coexist in the other group-IV semiconductors with the diamond-type structure, i.e. in Ge and in diamond itself, as well as in two III–V compounds with the zinc-blende structure, namely GaAs and GaP. For the present purposes, we also reproduce in table 1 the $\rm Mu^0_T$ parameters for the II–VI compounds ZnS and ZnSe, but note that $\rm Mu^0_{BC}$ or other paramagnetic muonium states have *not* been observed in these two materials.

3.2. Shallow states: ZnO etc

The deep states contrast with muonium in ZnO where, as in CdS, the contact interaction is smaller than the free-muonium value by a factor of 10^{-4} [19]. This is undoubtedly the shallow donor state predicted by Van de Walle [18][4]. Here we envisage spin density spread over many atoms in a local accumulation of conduction band states. That is, the electron wavefunction is a superposition chiefly of Zn(4s) states with an envelope corresponding to a much dilated 1s function centred on the muon. An effective Bohr radius of 1.1 nm is consistent with the measured muon–electron contact interaction and with estimates in the hydrogenic shallow-donor model, using literature values of electron effective mass and dielectric constant.

The μSR spectrum for polycrystalline ZnO is reproduced in figure 1(a). It shows the characteristic hyperfine doublet as satellites placed symmetrically about the muon Larmor frequency. The central line corresponds to muons which either fail to pick up an electron on implantation or which reach some other diamagnetic state. A small degree of anisotropy of the muon–electron hyperfine interaction is visible as a characteristic powder-pattern lineshape—the two satellites appearing as the mirror images. Evidently the smallest (inner) splitting corresponds to $A_\perp$, since this carries maximum weight in the powder pattern, and the largest (outer) splitting corresponds to $A_\parallel$, which carries least weight. The inferred parameters are given in table 1 and a lineshape simulation (using these parameters without additional broadening) is superimposed as a dotted line on the experimental spectrum. The corresponding time-domain signal is shown in figure 1(c); here the theoretical powder-pattern response, rather than a superposition of Lorentzian lines, has been used for the first time in fitting the muon spin-rotation signal.

[4] Another form of molecular radical, in which most of the spin density is remote from the muon but localized on a small number of atoms, can reasonably be excluded in view of the low ionization temperature—see section 4.

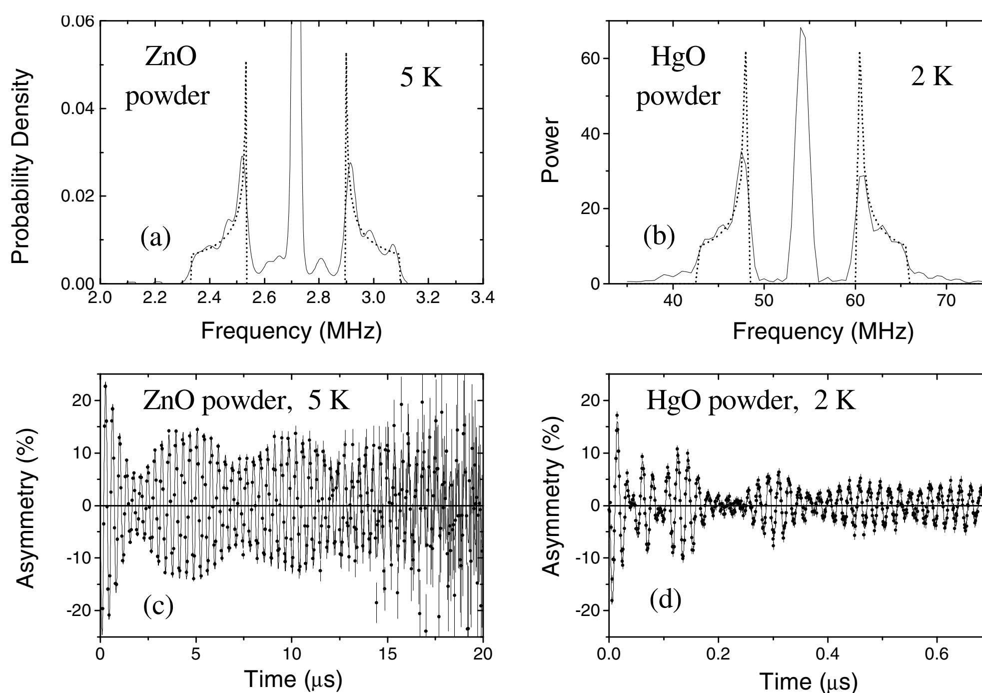

Figure 1. μSR frequency spectra for (a) ZnO and (b) HgO below the shallow-state ionization temperature, showing the hyperfine doublet satellites symmetrically placed around the muon Larmor frequency. Note the different frequency scales in (a) and (b). The corresponding time-domain signals and fits are given in (c) and (d).

The small anisotropy of the hyperfine parameters in ZnO may reflect the intrinsic anisotropy of electronic parameters in the hexagonal wurtzite structure. Otherwise it may indicate an admixture of atomic orbitals other than Zn(4s) and perhaps provide some clue to the precise muon site and nature of the local bonding. We hope in due course to map the electron distribution via superhyperfine interactions with the (4% abundant) ^{67}Zn nuclei.

It is noteworthy that our present data for polycrystalline CdO show a tantalizing glimpse of a shallow muonium state similar to that in ZnO and the other Cd chalcogenides. However, its μSR spectrum is at the limit of detectability, with the satellite lines faint in comparison with the diamagnetic central line, and we have so far been unable to make a reliable characterization. In the following sections we present the unmistakably strong signals of paramagnetic muonium in HgO, which account for some 80% of the implanted muons in this material, expanding on our preliminary account [26] and including new longitudinal-field data.

3.3. A new intermediate state in HgO

The μSR spectrum for polycrystalline HgO is reported in figure 1(b), again with the a powder lineshape simulation superimposed on the figure. The apparent resemblance of figures 1(a) and 1(b) belies very different frequency scales. Thus the ZnO spectrum spans a total width of only 800 kHz whereas the HgO spectrum[5] spans 25 MHz. The inferred hyperfine parameters

[5] The ZnO spectrum of figure 1(a) was recorded at the ISIS pulsed muon source (EMU instrument) whereas the higher frequencies involved for HgO required that of figure 1(b) to be recorded at the continuous source at PSI (GPS Instrument). The data of figure 2 are time-averaged muon-polarization data, recorded at ISIS (DEVA instrument).

are greater in the same ratio, as entered in table 1. They fall in a range which permits an interesting check on their values by means of repolarization measurements in longitudinal magnetic fields. The principle of these may be understood from the energy-level scheme in the inset to figure 2. This resembles the Breit–Rabi scheme for atomic hydrogen with two important distinctions: the low contact interaction puts the relevant ($\Delta M = 1$) level crossing at the readily accessible field of $H_{res} \sim \pi A_{iso}/\gamma_\mu = 55$ mT and the anisotropy of the hyperfine interaction causes the crossing to be avoided: that is, the degeneracy which would exist for a purely scalar interaction $A_{iso}\boldsymbol{I} \cdot \boldsymbol{S}$ is lifted and the resultant mixing of electron ($\boldsymbol{S}$) and muon ($\boldsymbol{I}$) spin states causes a resonant dip in time-average muon polarization. Figure 2 shows the form of this resonance for polycrystalline HgO at several temperatures. A powder-pattern lineshape is discernible at the lower temperatures and may be compared with the characteristic cusp for Mu^0_{BC} in polycrystalline Si, where the corresponding resonance falls at the much higher field of 0.32 T [27]. At the higher temperature, motional narrowing to a more symmetrical resonance is apparent, implying some diffusion of the centre, either locally or long range.

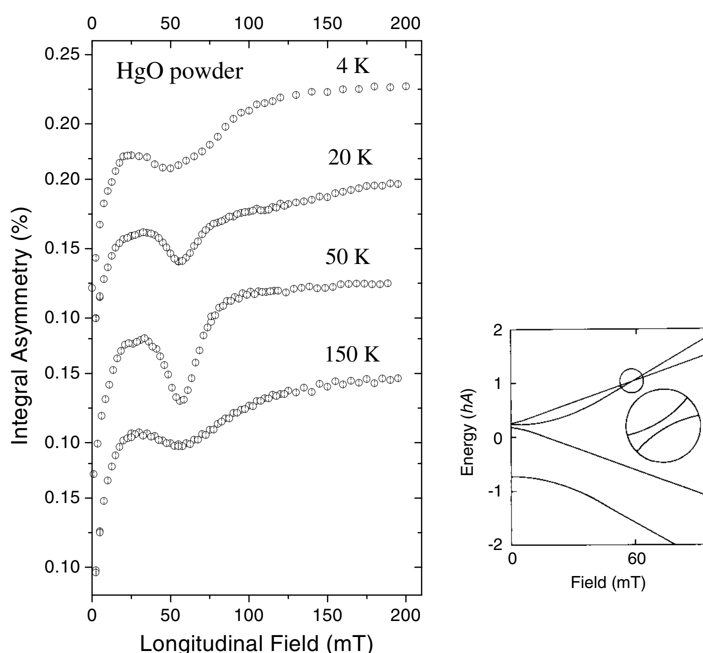

Figure 2. Time-average muon polarization as a function of field at four temperatures for HgO, showing the avoided level-crossing resonance at ∼60 mT. Inset: a schematic Breit–Rabi energy-level diagram for the anisotropic muonium state in HgO.

The hyperfine parameters for HgO are seen in table 1 to be far too large for a shallow hydrogenic donor. They are in fact more akin to those of Mu^0_{BC} in Si—the compact molecular radical state. This is also true of its ionization temperature and binding energy, entered in table 2, as we now describe.

4. Temperature dependences: binding energies and donor levels

In the ionization régimes, the amplitudes of the diamagnetic signals—the central lines at the muon Larmor frequency in the spectra of figure 1—grow at the expense of the paramagnetic

Table 2. Ionization parameters for muonium in ZnO and HgO, summarizing the analyses of figure 3, together with literature values [6–9] for Mu_{BC} in Si. T_{ion} is the ionization temperature for half signal amplitude, E_{ion} is the ionization energy and E_D the corresponding donor level below the conduction band edge, this latter assuming thermal equilibrium statistics. Also given for ZnO and Si are estimates of E_D^{hydr} for the binding energy of a hydrogenic shallow donor in the simple effective-mass theory (the relevant parameters are not reported for HgO).

	ZnO	HgO	Si (Mu_{BC})
T_{ion}/K	40	150	140
E_{ion}/meV	19 ± 1	136 ± 3	220 ± 10
E_D/meV	58 ± 6	300 ± 5	
E_D^{hydr}/meV	62		30

satellites. For both ZnO and HgO the sum of the diamagnetic and paramagnetic amplitudes remains approximately constant, accounting for the full incoming muon polarization. Figure 3 shows two methods by which these data may be treated. Figures 3(a) and 3(b) are simple Arrhenius plots for the incremental growth x (normalized to unity at high temperatures) of the diamagnetic signals for the two materials. Asymptotic linear fits as indicated yield ionization energies for the paramagnetic centres of $E_i = 19 \pm 1$ meV for ZnO and $E_i = 136 \pm 3$ meV

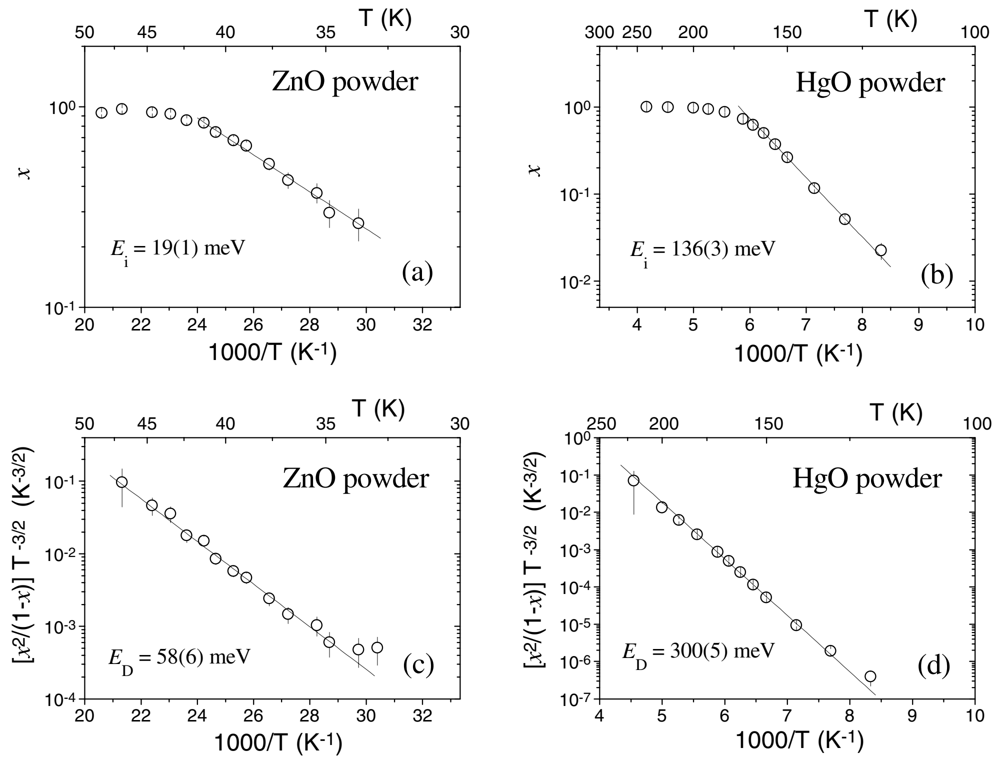

Figure 3. Arrhenius plots of the growth of the diamagnetic signal (x) versus reciprocal temperature for (a) ZnO and (b) HgO. An alternative treatment of the ionized (x) and unionized ($1 - x$) fractions which assumes thermal equilibrium (see the text) is given for ZnO and HgO in (c) and (d) respectively.

for HgO. This type of plot has been used previously for estimating the ionization energy of Mu_T^0 in Si and Ge and so must be used for comparing binding energies in the μSR literature, where these are commonly identified as the donor depths.

An alternative treatment, based on the assumption that thermodynamic equilibrium determines the relative fractions of ionized (x) and unionized ($1-x$) centres, gives directly the donor depths below the conduction band. This is illustrated by the plots in figures 3(c) and 3(d). The function $[x^2/(1-x)]T^{-3/2}$, plotted on the ordinates of these figures, is derived from the standard expression for the equilibrium free-electron concentration n in a doped and compensated n-type semiconductor, namely

$$\frac{n(n+N_A)}{N_D - N_A - n} = \frac{N_c}{2}\exp(-E_D/kT). \tag{3}$$

In this equation, E_D is the depth of the donor, N_D and N_A are respectively the donor and acceptor concentrations and N_c is the effective density of states in the conduction band, which is proportional to $T^{3/2}$. Writing $x = n/N_D$ and setting $N_A = 0$ (if acceptors are present we assume that electrons do not transfer to these without first being excited to the conduction band), equation (3) becomes

$$\frac{x^2}{1-x}T^{-3/2} = \text{constant} \times \exp(-E_D/kT). \tag{4}$$

A plot of the logarithm of the left-hand side of equation (4) versus $1/T$ thus yields the donor depth, E_D. The best fits to the data on these plots provide estimates of $E_D = 58 \pm 6$ meV for ZnO and $E_D = 300 \pm 5$ meV for HgO.

The first method is appropriate to direct promotion of the donor electron to the conduction band without detailed balance whereas the second takes into account the position of the Fermi energy: this latter tends to a value midway between the donor level and the conduction band edge in the limit of low temperature. At the present time, we are not able to decide which treatment of μSR data is appropriate, so care must be exercised in comparing donor depths from the muonium and hydrogen literature. The choice is not necessarily the same for the deep and shallow states or in different temperature ranges and should await a more detailed understanding of the electron capture and release processes occurring in the final stages of muon thermalization following implantation. We can, however, conclude with certainty that the depth of the donors associated with paramagnetic muonium is at least five times greater in HgO than in ZnO.

5. Questions: muon and proton sites, diffuse versus compact electron wavefunctions

Despite the precision of the spectroscopy, the muon site is not easily deduced from the hyperfine parameters. Both the obvious candidate sites, namely the bond centre and the site antibonding to oxygen, take their axial symmetry and principal axis from the original bond direction, so are not simply distinguished by symmetry. For ZnO, Van de Walle calculates that the interstitial proton has very similar energies at the two sites, with the bond centre marginally more stable. At or near the bond centre the charge defect is shared roughly equally between host anion and cation; at the antibonding site the resulting hydroxyl ion effectively changes the anion charge state: $O^{2-} + H^+ \rightarrow OH^-$. Can capture of an electron lead to weakly bound or shallow states at both sites? In CdS, above the ionization temperature, we find the muon to be at the antibonding site [17]; it presumably remains there on capturing an electron, so we favour the antibonding site as the centre for the shallow state, but this remains to be proven.

For the deeper state in HgO, the contact interaction A_{iso} indicates a spin density of 0.3% on the muon instead of 0.01% in ZnO and CdS. Most significantly—and here the analogy

with the Mu^0_{BC} centre in Si, Ge, GaAs and GaP is as striking as the similarity in ionization parameters—the large dipolar term $D = 5.2$ MHz indicates that most of the spin density is located close by. The effective muon–electron separation deduced from this parameter is about 0.4 nm in HgO, compared with 0.2 nm for Mu_{BC} in Si [22]. Assignment to the bond centre in HgO is therefore tempting, but sites antibonding to oxygen must again be considered. Inspection of the chain-like structure of HgO, depicted in figure 4, suggests that bridging sites between oxygens on adjacent chains might also be favourable. A consequence of the chain-like structure is that motion between adjacent sites, whether of the bond-centre or antibonding type, does not spherically average the hyperfine anisotropy. This allows observation of the level-crossing resonance of figure 2 at temperatures where the defect is clearly mobile, as we shall discuss in detail elsewhere.

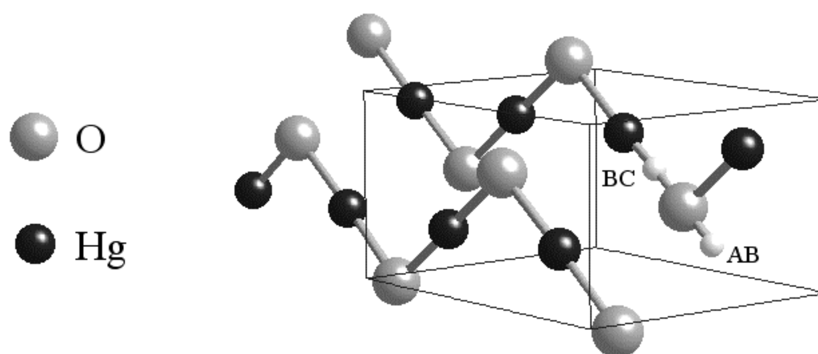

Figure 4. The structure of HgO with candidate muon sites near a bond centre (BC) or antibonding to oxygen (AB). This latter is drawn purely schematically: other possibilities exist nearby, e.g. sites which bridge to oxygens on adjacent chains.

For this new state in HgO, the notion of a trapped hydroxyl radical is also appealing, but this would have the wrong charge state for a donor and its muonium counterpart should have hyperfine parameters an order of magnitude higher again [28, 29]. Pending quantum chemical calculations for the muon or proton site and the accompanying singly occupied molecular orbital, we surmise simply that this latter is intermediate in spatial extent between that for Mu^0_{BC} in Si etc and that of the diffuse shallow state in ZnO.

The strange contrast between the deep states of various substitutional donors in ZnS and the shallow states of similar substituents in CdS has long been recognized. Reviewing the data available in 1975, Stoneham writes ‘It is not yet possible to predict the behaviour in advance’ [30]. This appears still to be the case, and no single parameter (structure, ionicity, band-gap) provides a reliable guide. The newer data for interstitial muonium show some similar trends, with a deep state in ZnS and shallow states in CdS and ZnO—but now also the additional puzzle of an intermediate state in HgO. It may be hoped that characterization of muonium, as a centre that may be created by muon implantation with equal facility in all the II–VI compounds as well as other materials, may provide the necessary systematics to elucidate this long-standing problem.

Acknowledgments

The EPSRC (via GR/R25361), the PRAXIS XXI Programme and the European Union Framework V Access to Research Infrastructures Programme are gratefully acknowledged for funding.

References

[1] Jones R, Coomer B J, Goss J P, Hourahine B and Resende A 2000 *Special Defects in Semiconducting Materials (Diffusion and Defect Data: Solid State Data. Part B: Solid State Phenomena, vol 71)* ed R P Agarwala (Zurich: Trans Tech)
[2] Holm B, Bonde Nielsen K and Bech Nielsen B 1991 *Phys. Rev. Lett.* **66** 2360
[3] Johnson N M, Herring C and Van de Walle C 1994 *Phys. Rev. Lett.* **73** 130
[4] Bonde Nielsen K, Bech Nielsen B, Hanson J, Andersen E and Andersen J U 1999 *Phys. Rev.* B **60** 1716
[5] Seager C H, Anderson R A and Estreicher S K 1995 *Phys. Rev. Lett.* **74** 4565
[6] Patterson B 1988 *Rev. Mod. Phys.* **60** 69 and references therein
[7] Kreitzman S R, Hitti B, Lichti R L, Estle T L and Chow K H 1995 *Phys. Rev.* B **51** 13 117
[8] Hitti B, Kreitzman S R, Estle T L, Bates E S, Dawdy M R, Head T L and Lichti R L 1999 *Phys. Rev.* B **59** 4918
[9] Lichti R L 1995 *Phil. Trans. R. Soc.* A **350**
[10] Estreicher S K 1987 *Phys. Rev.* B **36** 9122
[11] Déak P, Snyder L C and Corbett J W 1988 *Phys. Rev.* B **37** 6887
[12] Briddon P R and Jones R 1990 *Hyperfine Interact.* **64** 593
[13] Van de Walle C G, Denteneer P J H, Bar Yam Y and Pantelides S T 1989 *Phys. Rev.* B **39** 10 791
[14] Watkins G W 1981 *Defects in Semiconductors (Proc. MRS vol 2)* (Amsterdam: North-Holland) p 21
[15] Thomas D G and Lander J J 1956 *J. Chem. Phys.* **25** 1136
[16] Hutson A R 1957 *Phys. Rev.* **108** 222
[17] Gil J M, Alberto H V, Vilão R C, Piroto Duarte J, Mendes P J, Ferreira L P, Ayres de Campos N, Weidinger A, Krauser J, Niedermayer Ch and Cox S F J 1999 *Phys. Rev. Lett.* **83** 5294
[18] Van de Walle C J 2000 *Phys. Rev. Lett.* **85** 1012
[19] Cox S F J, Davis E A, Cottrell S P, King P J C, Lord J S, Gil J M, Alberto H V, Vilão R C, Piroto Duarte J, Ayres de Campos N, Weidinger A, Lichti R L and Irvine S J C 2001 *Phys. Rev. Lett.* **86** 2601
[20] Cox S F J 1995 *Phil. Trans. R. Soc.* A **350** 171
[21] Brewer J H, Crowe K M, Johnson R F, Patterson B D, Fleming D G and Schenck A 1973 *Phys. Rev. Lett.* **31** 143
[22] Cox S F J and Symons M C R 1986 *Chem. Phys. Lett.* **126** 516
[23] Kiefl R F *et al* 1988 *Phys. Rev. Lett.* **60** 224
[24] Gorelinskii Yu V and Nevinnyi N N 1987 *Sov. Tech. Phys. Lett.* **13** 45
[25] Bech Nielsen B *et al* 1994 *Mater. Res. Forum* **143–7** 909
[26] Gil J M, Alberto H V, Vilão R C, Piroto Duarte J, Ayres de Campos N, Weidinger A, Davis E A and Cox S F J 2001 *J. Phys.: Condens. Matter* submitted
[27] Cooke D W, Leon M, Paciotti M A, Meier P F, Cox S F J and Davis E A 1994 *Phys. Rev.* B **50** 4391
[28] Claxton T A, Graham A M, Cox S F J, Maric Dj M, Meier P F and Vogel S 1990 *Hyperfine Interact.* **65** 913
[29] Brivati J A, Symons M C R, Tinling D and Wardate H 1967 *Trans. Faraday Soc.* **63** 2112
[30] Stoneham A M 1975 *Theory of Defects in Solids* (Oxford: Oxford University Press)